Supramolecular Chemistry

DOI: 10.1002/anie.201402042

A Collection of Fullerenes for Synthetic Access Toward Oriented Charge-Transfer Cascades in Triple-Channel Photosystems**

Altan Bolag, Javier López-Andarias, Santiago Lascano, Saeideh Soleimanpour, Carmen Atienza, Naomi Sakai, Nazario Martín, and Stefan Matile**

Abstract: *The development of synthetic methods to build complex functional systems is a central and current challenge in organic chemistry. This goal is important because supramolecular architectures of highest sophistication account for function in nature, and synthetic organic chemistry, contrary to high standards with small molecules, fails to deliver functional systems of similar complexity. In this report, we introduce a collection of fullerenes that is compatible with the construction of multicomponent charge-transfer cascades and can be placed in triple-channel architectures next to stacks of oligothiophenes and naphthalenediimides. For the creation of this collection, modern fullerene chemistry—methanofullerenes and 1,4-diarylfullerenes—is combined with classical Nierengarten–Diederich–Bingel approaches.*

Biological function originates from supramolecular architectures of highest sophistication.[1] No one knows what could be found if functional materials of similar sophistication could be synthesized with similar precision because the ability to do so remains rudimentary, despite enormous efforts worldwide.[1–9] To help improve on this situation, we became interested in developing synthetic methods to grow complex architectures directly on solid surfaces.[10–17] This approach is important to ensure directionality, which is a critical issue to, for example, construct oriented multicomponent antiparallel redox gradients (OMARGs) which drive holes and electrons in opposite directions after their generation with light,[14] thus resembling biological photosystems.[1]

Toward this general objective, zipper assembly, a sticky-end-layer-by-layer method, has been introduced.[10] The discovery of surface-initiated ring-opening disulfide-exchange polymerization as a most convenient approach to complex architectures followed.[11,12] Based on this robust, somewhat bioinspired method, self-organizing surface-initiated polymerization (SOSIP) was conceived to grow charge-transporting π stacks on indium tin oxide (ITO).[11] To adapt SOSIP to the synthesis of multicomponent architectures with two[14–16] or three[17] coaxial charge-transporting channels, templated self-sorting (TSS) during co-SOSIP[13] and templated stack exchange (TSE, Figure 1) after SOSIP[14–17] were introduced next. Sometimes referred to as supramolecular n/p heterojunctions (SHJs),[3] surface architectures with coaxial channels to transport holes and electrons are of interest for maximizing photoinduced charge separation without losses in charge mobility.

Initial efforts to use the SOSIP-TSE methodology for the synthesis of the first OMARG-SHJ architectures focused exclusively on naphthalenediimides (NDIs).[14] However, in today's functional supramolecular materials, fullerenes[4–8] and oligothiophenes[9] are considered as most powerful components for the construction of hole- and electron-transporting channels. By combining classics with recent progress in fullerene chemistry, that is, Nierengarten–Diederich–Bingel fullerenes,[5] methanofullerenes,[6] and 1,4-diarylfullerenes,[7] we herein report the design, synthesis, and evaluation of a collection of fullerenes which 1) are compatible with the construction of charge-transfer cascades, that is, multicomponent OMARGs, and 2) can be placed, with molecular-level precision, next to oligothiophene stacks in operational triple-channel architectures.

For compatibility with SOSIP-TSE, the fullerenes **F** have to offer an aldehyde and good solubility in aprotic polar solvents (Figure 1). The double Bingel fullerene **DBF** has been shown previously, in a different context, to fulfill these prerequisites.[15] The **SBF** (single Bingel fullerene), with only one cyclopropane ring, was expected to have about a 0.06 eV lower HOMO and LUMO energy level compared to those of **DBF** (Figure 2).[5] In **SBF**, the central benzaldehyde and both triethyleneglycol (TEG) solubilizers are preserved (solubility with only one TEG was insufficient). To raise the HOMO/LUMO levels from those of **DBF**, the recently disclosed methanofullerenes were considered.[6] **DBMF** and **SBMF**,

[*] Dr. A. Bolag,[+] S. Lascano,[+] S. Soleimanpour, Dr. N. Sakai, Prof. S. Matile
Department of Organic Chemistry, University of Geneva
Geneva (Switzerland)
E-mail: stefan.matile@unige.ch
Homepage: http://www.unige.ch/sciences/chiorg/matile/
J. López-Andarias,[+] Dr. C. Atienza, Prof. N. Martín
Departamento de Química Orgánica, Universidad Complutenese
Madrid (Spain)
and
IMDEA Nanoscience, Madrid (Spain)
E-mail: nazmar@quim.ucm.es
[+] These authors contributed equally to this work.

[**] We thank J.-F. Nierengarten for advice, A. Sobczuk, H. Hayashi, and L. Cervini for contributions to synthesis, the NMR and Mass Spectrometry platforms for services, and the University of Geneva, the European Research Council (ERC Advanced Investigator), the National Centre of Competence in Research (NCCR) Chemical Biology and the Swiss NSF for financial support (S.M.). We also thank the European Research Council ERC-2012-ADG (Chirallcarbon), Ministerio de Economía y Competitividad (MINECO) of Spain (project CTQ2011-24652; Ramón y Cajal granted to C.A. and FPU granted to J.L.-A.) and the CAM (MADRISOLAR-2 project S2009/PPQ-1533; N.M.). N.M. is indebted to the Alexander von Humboldt Foundation.

Supporting information for this article is available on the WWW under http://dx.doi.org/10.1002/anie.201402042.

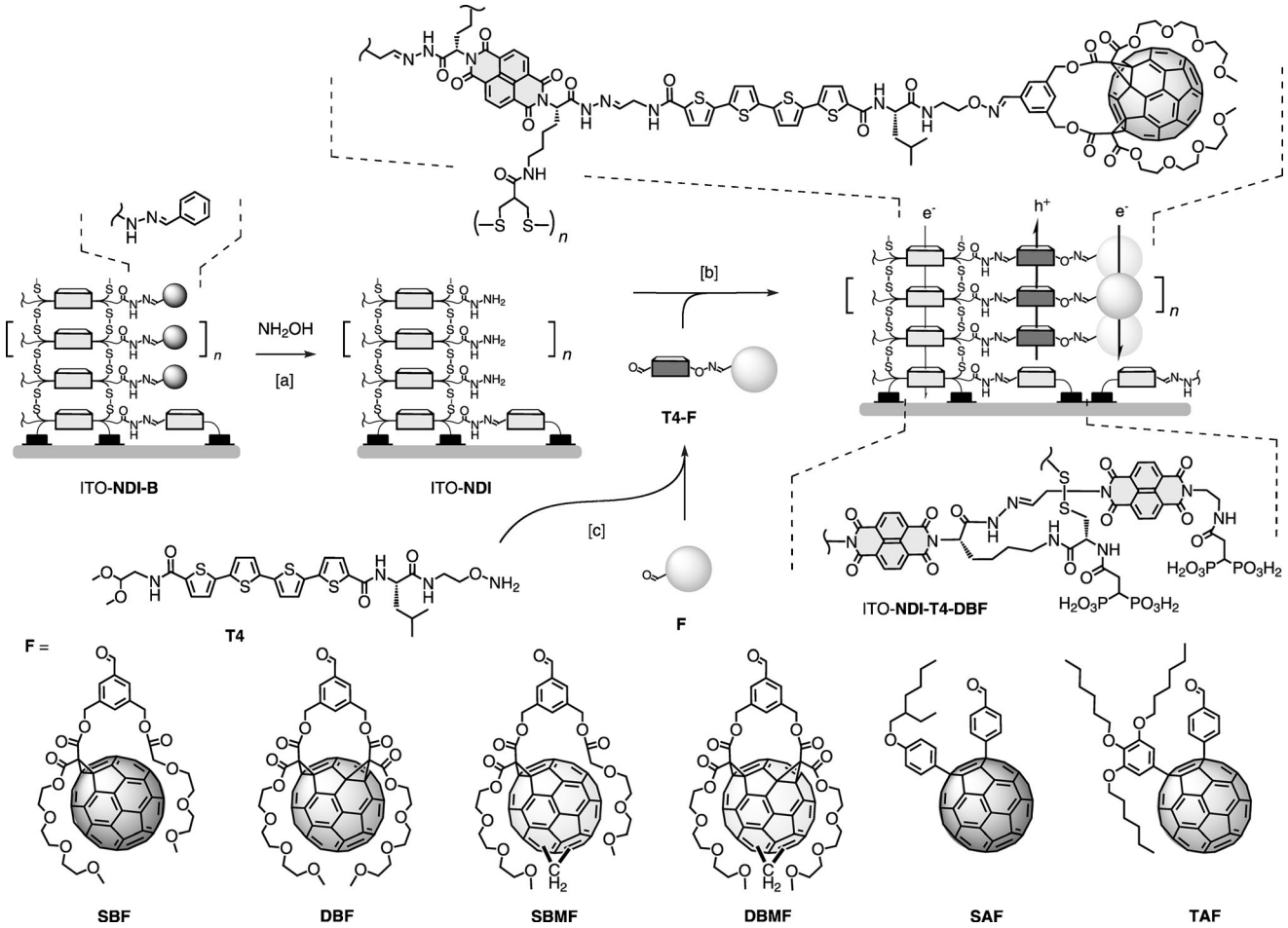

Figure 1. Structure of the fullerenes **F** and their incorporation into triple-channel architectures, for example, ITO-**NDI-T4-DBF. SBMF** and **DBMF** are mixtures of regioisomers. [a,b] Templated stack exchange (TSE); for yields, see Table 1. [c] For synthesis of **T4-F**, see Scheme 1.

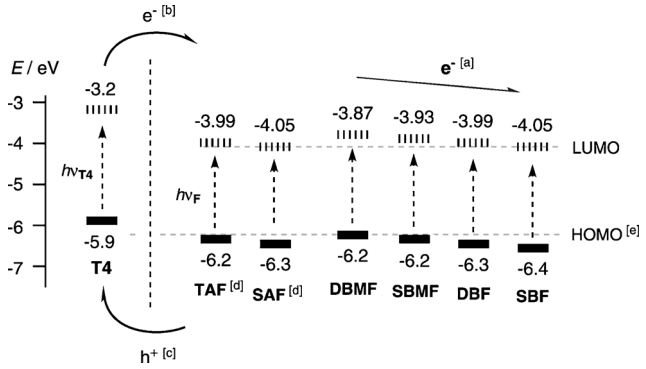

Figure 2. Energy levels of HOMO (bold) and LUMO (dashed) of the fullerenes **F** and **T4**[15] (in eV against vacuum, assuming −5.1 eV for Fc^+/Fc [compare Figures 1 (structures) and 3 (DPVs)]. [a] Gradually decreasing LUMO levels designed to build oriented gradients into the electron (e^-) transporting fullerene channels in, for example, triple-channel architectures of ITO-**NDI-T4-DBF** (Figure 1). Charge separation between the co-axial **T4-F** stacks can occur by [b] e^- transfer after excitation of **T4** ($h\nu_{T4}$) and [c] h^+ transfer after excitation of **F** ($h\nu_F$). [d] Measured for the methyloxime derivatives.[18] [e] The HOMO levels of **F**, estimated from the gradual onset of their absorption, are affected by non-negligible uncertainty [LUMO levels, from DPV (Figure 3), are accurate].

accessible as regioisomeric mixtures from Bingel reaction of methanofullerenes with the same malonates, should reproduce the energy difference between **DBF** and **SBF** at a higher level. To more profoundly modulate the HOMO/LUMO levels of fullerenes, the recently introduced direct coupling with phenyl rings appeared most promising.[7] The comparison between the electron-richer **TAF**, having three alkoxy substituents, and the electron-poorer **SAF**, having only one alkoxy substituent, was expected to clarify the potential of this alternative approach.

The oligothiophene-fullerene dyad **T4-SBF** was synthesized as follows (Scheme 1).[18] The diol **1**,[5] obtained from the triester **2** by a more user-friendly pathway,[19] was converted into the malonate **3** by consecutive esterification with the TEG-glycolate **4** and TEG-malonate **5**. Cyclopropanation of the fullerene **6** with **3** gave the Bingel fullerene **7**, which was deprotected to yield the desired **SBF**. The quaterthiophene **8** was prepared from the bithiophene **9** and bromothiophene **10** as described.[16]

The diacid **8** was first coupled with the amine **11**—equipped with an essential leucine spacer to assure good solubility—and then with amine **12** (Scheme 1). Chemoselective Alloc removal liberated the reactive alkoxyamine in

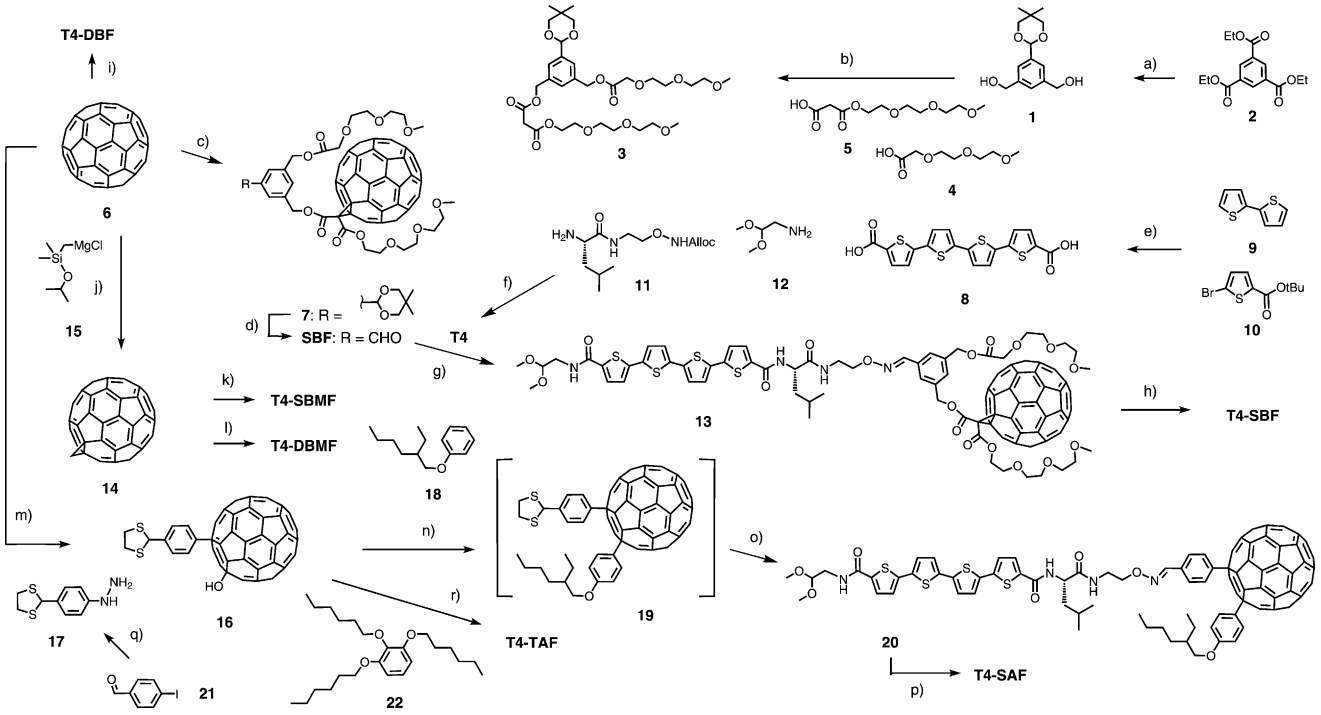

Scheme 1. Synthesis of the fullerene collection. a) 1. $LiBH_4$, THF, 60%; 2. PCC, 99%; 3. 2,2-dimethyl-1,3-propanediol, *p*-TsOH, 86%; 4. $LiAlH_4$, THF, 57%;[19] b) 1. **1**, **4**, EDC, DMAP, CH_2Cl_2, 67%; 2. same with **5**, 66%; c) **3**, I_2, DBU, 64%; d) TFA, RT, 4 h, 52%; e) 1a. **9**, *n*BuLi; 1b. Bu_3SnCl; 2. **10**, $[Pd(PPh_3)_4]$, 82%; 3. TFA, RT, quant;[16] f) 1. **8**, **11**, HBTU, TEA, 46%; 2. same with **12**, 42%; 3. $[Pd(PPh_3)_2Cl_2]$, Bu_3SnH; g) AcOH, RT, 15 min, quant; h) TFA, quant; i) as for **T4-SBF** (g, h) with **DBF**;[15] j) 1. DMF, ODCB, 89%; 2a. *t*BuOK, ODCB; 2b. $CuCl_2$, 100 °C, 12 h, 79%;[6] k) as for **T4-SBF** with **14** (c, d, g, h); l) as for **T4-DBF** with **14** (i); m) **17**, $NaNO_2$, HCl, O_2, 15%; n) **18** (from phenol, rac 2-ethylhexylbromide, *t*BuOK, 98%), *p*-TsOH, 80 °C; o) 1. HgO, BF_3, 10% (2 steps); 2. **T4**, AcOH, RT, 15 min, 47%; p) TFA, 72%; q) 1. 1,2-ethanedithiol, $BF_3{\cdot}Et_2O$, 96%; 2. *t*Bu carbazate, CuI, phenanthroline, Cs_2CO_3, 67%; 3. HCl, quant; r) 1. **22** (from pyrogallol, *n*-hexylbromide, K_2CO_3, 76%), *p*-TsOH, 80 °C; 2. HgO, BF_3, 28% (2 steps); 3. **T4**, AcOH, RT, 15 min, 52%; 4. TFA, 93%. DBU = ,8-diazabicyclo[5.4.0]undec-7-ene, DMAP = 4-(*N*,*N*-dimethyl)pyridine, DMF = *N*,*N*-dimethylformamide, EDC = 1-ethyl-3-(3-dimethylaminopropyl)carbodiimide, HBTU = O-benzotriazole-*N*,*N*,*N*′,*N*′-tetramethyluronium-hexafluoro phosphate, ODCB = *o*-dichlorobenzene, PCC = pyridnium chlorochromate, TFA = trifluoroacetic acid, THF = tetrahydrofuran, Ts = 4-toluenesulfonyl.

T4. Spontaneous oxime formation between **T4** and **SBF** then gave the dyad **13** essentially in situ. Aldehyde deprotection afforded the desired dyad **T4-SBF** under mild reaction conditions, and made ready for TSE with the activated ITO-**NDI** architecture (Figure 1). **T4-DBF** was prepared following the exceptionally mild procedure developed for **T4-SBF**.

The fullerene **14**, having a very small 1,2-dihydromethano group, was synthesized using the original procedure.[6] Namely, addition of the Grignard reagent **15** and subsequent deprotonation of the obtained silylfullerene and oxidative cyclopropane formation in the presence of $CuCl_2$ at 100 °C. The fullerene **14** was converted into **T4-SBMF** and **T4-DBMF** by using the procedure described above for the complementary **T4-SBF** and **T4-DBF**.

The introduction of dithiane-protected benzaldehydes into the fullerenol **16** turned out to be feasible (Scheme 1). The Wang reaction with the phenyl hydrazine **17** in the presence of $NaNO_2$ gave the desired product **16** in, at least in this context, very reasonable 15% yield. The 1,4-addition was completed with the alkoxybenzene **18** in the presence of *para*-toluenesulfonic acid (*p*-TsOH), and HgO-mediated hydrolysis of the non-isolable intermediate **19** gave the key product **SAF** (Figure 1). Incubation of **SAF** with **T4** gave the dyad **20** in situ, and mild acidic deprotection afforded **T4-SAF**, the dyad needed for stack exchange with ITO-**NDI**. The hydrazine **17** was readily accessible from *p*-iodobenzaldehyde (**21**) in a three-step synthetic procedure.[18] The alkoxybenzene **18** was prepared by simple alkylation of the corresponding phenol. **T4-TAF**, the electron-rich homologue of **T4-SAF**, was prepared analogously from **16** using the alkylated pyrogallol **22** instead of **18**.

The redox potential values for all fullerenes were determined by cyclic voltammetry (CV) and differential pulse voltammetry (DPV). LUMO energy levels against vacuum were estimated assuming −5.1 eV for Fc^+/Fc (Figure 2).[20] For the Bingel quartet **DBMF**, **SBMF**, **DBF**, and **SBF**, a marvelous stepwise decrease of the LUMO energies by 60 meV each could be detected unambiguously by DPV against Fc^+/Fc as the internal standard (Figure 3). This finding provided experimental support that the Bingel methanofullerene series is suitable for the synthesis of four-component electron-transfer cascades in complex architectures.

For DPV measurements, **SAF** and **TAF** were converted into their respective methyloximes. This transformation of the aldehyde acceptors into formal N-alkoxyimine donors raised the LUMO levels, but only slightly. Consistent with the presence of fewer alkoxy donors, the LUMO level of **SAF** was

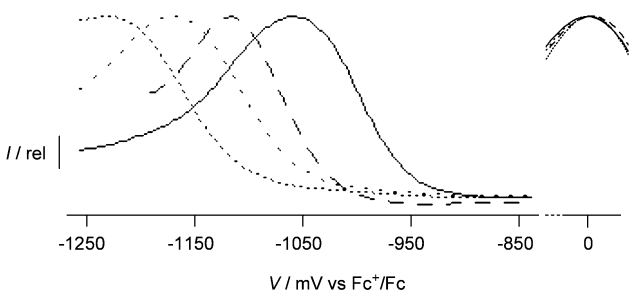

Figure 3. DPVs of **DBMF**, **SBMF**, **DBF**, and **SBF** (left to right), measured in CH_2Cl_2 against internal Fc^+/Fc standards at 0 mV.

−60 meV below that of **TAF** (Figure 2). The HOMO energies of none of the fullerenes could be directly measured by DPV, and an accurate estimation from the HOMO/LUMO gap in the absorption spectra is difficult because of the weak and gradually decreasing tail reaching up to about 650 nm. A constant HOMO/LUMO gap of 2.3 eV was assumed based on the literature.[21] For **SAF** and **TAF**, the HOMO/LUMO gap was arbitrarily reduced to 2.2 eV considering the previously reported[7a] red shift caused by their lowered symmetry (Figure 2). The direct determination of the LUMO energy levels of the fullerenes, of central importance for this study, is most accurate (Figure 3 and Figure S2 in the Supporting Information), while the intrinsic uncertainty of the absolute values of the HOMO energy levels is inconsequential.

To explore the compatibility of the new fullerenes with triple-channel architectures, original NDI stacks were grown by the established disulfide-exchange SOSIP on ITO in the presence of NDI templates on the surface and benzaldehyde hydrazone templates along the stacks.[14] The absorption of the obtained ITO-**NDI-B** was kept constant around $A_{380} \approx 0.17$ at the low-energy maximum of the NDI stack at $\lambda =$ 380 nm (Figure 4d). This constant $A_{380} \approx 0.17$ was important to maximize comparability of the results. In an ideal architecture, $A_{380} \approx 0.17$ corresponds to about 142 NDIs stacked on top of each other, or a formal thickness of about 47 nm. The orthogonal dynamic covalent chemistry[22] of TSE[14] is the key to cleaving the hydrazones along the NDI stacks in ITO-**NDI-B** with excess hydroxylamine (Figure 1). The large pores left behind in ITO-**NDI** with reactive hydrazides along their walls were then filled with the **T4-F** and control **T4-C** with an oxime from 4-*tert*-butyl benzaldehyde in place of the fullerene (see Scheme S3 in the Supporting Information). In the absorption spectrum of ITO-**NDI-T4-SBF**, the presence of all components was clearly observable (Figures 4a,c,d). From the absorption spectra, a TSE yield of 67% was estimated (Table 1, entry 1). The formation of all other triple-channel architectures occurred with similar satisfactory yield (Table 1). Only the control architecture ITO-**NDI-TAF** (compound lacking the **T4** moiety) was obtained with a low 33% yield, presumably because the accommodation of the bulky fullerenes in close proximity to the NDI stack was hindered.

Photocurrent generation of the triple-channel architectures was measured under routine conditions with the photosystems as the working electrode, a platinum wire as the counter electrode, and triethanolamine (TEOA) as sacrificial mobile hole transporter. Other, also reversible, hole carriers were applicable but gave lower currents. While results obtained under these conditions are not comparable with those from optimized optoelectronic devices, they are suitable to evaluate and compare different multicomponent architectures. The highest currents were observed for ITO-**NDI-T4-SBF** (Figure 5a, Table 1, entry 1). This is the most active triple-channel photosystem prepared so far.[17] With a distinct shoulder around $\lambda = 430$ nm, the action spectrum demonstrated that the oligothiophenes contribute to photocurrent generation (Figure 4a, dashed line). With absorption and action spectra of fullerenes and NDIs being very weak above $\lambda = 400$ nm, the action spectrum of ITO-**NDI-T4-SBF** demonstrated that these contributions of the oligothiophenes are highly significant (Figure 4a, dashed gray lines). High activity below $\lambda = 400$ nm indicated that fullerenes and NDIs also

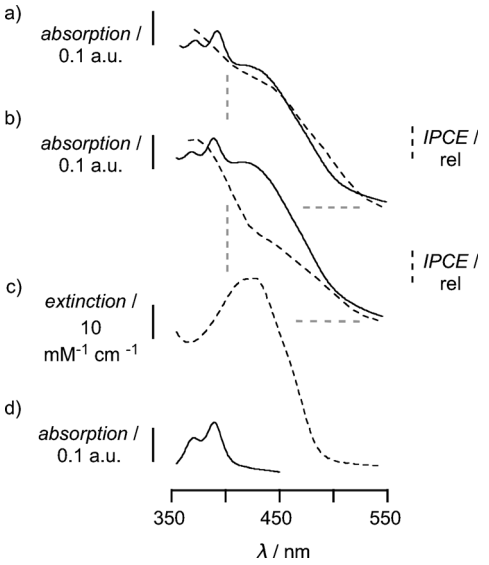

Figure 4. Action spectra of a) ITO-**NDI-T4-SBF** and b) ITO-**NDI-T4-SBMF** (dashed lines) compared to their absorption spectra (solid lines) and those of c) **T4-SBF** in DMSO and d) ITO-**NDI**. The grey dashed lines in a) and b) mark the area where photocurrent is mostly generated by **T4**.

Table 1: Characteristics of triple-channel photosystems.

	Photosystem[a]	TSE [%][b]	J_{SC} [$\mu A\,cm^{-2}$][c]	ΔE_{HOMO} [eV][d]	ΔE_{LUMO} [eV][e]
1	ITO-**NDI-T4-SBF**	67	12.0	+0.5	−0.85
2	ITO-**NDI-T4-DBF**	89	8.8	+0.4	−0.79
3	ITO-**NDI-T4-SBMF**	78	2.1	+0.3	−0.73
4	ITO-**NDI-T4-DBMF**	62	2.2	+0.3	−0.67
5	ITO-**NDI-T4-SAF**	82	3.9	+0.4	−0.85
6	ITO-**NDI-T4-TAF**	70	2.8	+0.3	−0.79
7	ITO-**NDI-T4-C**	90	2.4	–	–

[a] See Figure 1 for structures.[18] [b] Yield for templated stack exchange, estimated from absorption spectra, see Figure 4. [c] Short-circuit photocurrent density generated by irradiation with white light (solar simulator, $W = 100$ mW, 50 mM TEOA, 0.1 M Na_2SO_4, Pt counter electrode). [d] Energy difference to the HOMO of **T4** (from DPV, compare Figure 2 and 3). [e] Energy difference from the LUMO of **T4**.

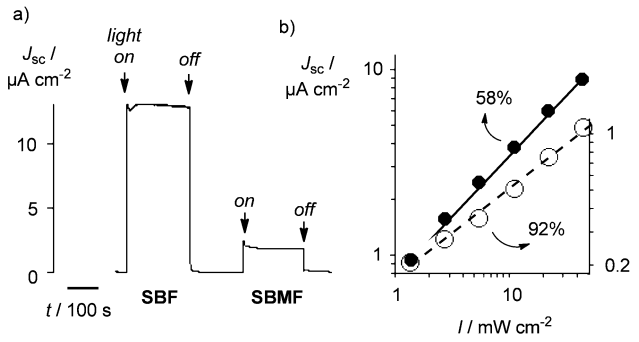

Figure 5. a) Photocurrent generated by ITO-**NDI-T4-SBF** (left) and ITO-**NDI-T4-SBMF** (right, $W = 100$ mW, 50 mM TEOA, 0.1 M Na_2SO_4, Pt). b) Dependence of the short-circuit current density J_{SC} on the light intensity I for ITO-**NDI-T4-SBF** (●) and ITO-**NDI-T4-SBMF** (○), with curve fit and bimolecular charge recombination efficiencies η_{BR} determined from the slope.[18]

contribute to photocurrent generation (Figure 4a). For comparison, the fullerene-free double-channel control ITO-**NDI-T4-C** was prepared with a record TSE yield of 90% (probably as a result of reduced steric demand; Table 1, entry 7). Photocurrent generation by ITO-**NDI-T4-C** never exceeded $J_{SC} = 2.4\ \mu A\,cm^{-2}$. The presence of an electron-transporting **SBF** channel next to the hole-transporting **T4** channel in ITO-**NDI-T4-SBF** thus caused a greater than fivefold increase in activity, although the TSE yield and thus the relative **T4** content was with 67% clearly lower than in the fullerene-free control ITO-**NDI-T4-C** (Table 1, entry 1 versus 7). This result confirmed the significance of operational triple-channel architectures.

High photocurrents were also found for ITO-**NDI-T4-DBF**, whereas the 1,4-diarylfullerenes containing ITO-**NDI-T4-SAF** and ITO-**NDI-T4-TAF** were less active, and ITO-**NDI-T4-SBMF** and ITO-**NDI-T4-DBMF** with methanofullerenes were worst (Figure 5a; Table 1, column 2). Bimolecular charge recombination efficiencies were determined from the dependence of the photocurrent generation on the intensity of irradiation as described.[14] The most active ITO-**NDI-T4-SBF** gave $\eta_{BR} = 58\%$ (Figure 5b; ●), whereas in the least active ITO-**NDI-T4-SBMF**, recombination was very high with $\eta_{BR} = 92\%$ (Figure 5b, ○). This difference suggested that when compared to Bingel fullerenes, the poor activity observed for methanofullerenes could stem from poor charge mobility. The organization of strings of methanofullerenes and, although less pronounced, also of 1,4-adducts in triple-channel architectures could be hindered by the random location of the third cylcopropane ring and the clumsy diaryl substituents, respectively. Moreover, poor electron transfer from excited oligothiophenes to fullerenes with high LUMO could also reduce activity (Table 1, column 4). The weak photocurrent generation by the oligothiophenes in the action spectrum of ITO-**NDI-T4-SBMF**, compared to that of ITO-**NDI-T4-SBF**, was in support of this interpretation (Figure 4a versus b: dashed lines). The same could be said for poor hole transfer from excited fullerenes with high HOMO to oligothiophenes (Table 1, column 3). The weaker activities of ITO-**NDI-T4-SAF** and ITO-**NDI-T4-TAF** compared to ITO-**NDI-T4-SBF** and ITO-**NDI-T4-DBF** with identical LUMO but lower HOMO could be explained by reduced hole transfer (Table 1). The decisive importance of hole transfer from excited fullerenes has been suggested for other systems.[8] Taken together, the origin of the observed trends are presumably quite complex, and electron transfer and hole transfer, as well as charge mobility and charge recombination might all contribute to the final photocurrent, although electron transfer from excited oligothiophenes to fullerenes is probably most relevant (Figure 4a versus b).

In summary, this study introduces a collection of fullerenes which is compatible with the construction of triple-channel photosystems having oriented strings of different fullerenes for directional electron transfer along multicomponent gradients, similar to biological photosystems. The redox potentials of the fullerenes could be adjusted without losses in reactivity and solubility by combining cutting-edge fullerene chemistry with classical Nierengarten–Diederich–Bingel strategies. Confirmed compatibility with SOSIP-TSE methodology provided exceptionally mild, fast, and easy conditions for the directional positioning of the new fullerenes in triple-channel architectures with molecular-level precision. The obtained multicomponent surface architectures are as sophisticated as it gets today, and the reported activities include the best observed so far with triple-channel photosystems. Charge recombination efficiencies larger than 50% are important because they demonstrate that future suppression of charge recombination with antiparallel redox gradients could further increase activity and would be easily detectable.[14] To achieve this general objective, the redox engineering of oligothiophene stacks will be required next, preliminary results are promising and will be reported in due course.

Received: February 3, 2014
Published online: April 1, 2014

Keywords: charge transfer · fullerenes · hydrazones · polymerization · supramolecular chemistry

[1] R. Bhosale, J. Míšek, N. Sakai, S. Matile, *Chem. Soc. Rev.* **2010**, *39*, 138–149.
[2] a) T. Aida, E. W. Meijer, S. I. Stupp, *Science* **2012**, *335*, 813–817; b) D. M. Bassani, L. Jonusauskaite, A. Lavie-Cambot, N. D. McClenaghan, J.-L. Pozzo, D. Ray, G. Vives, *Coord. Chem. Rev.* **2010**, *254*, 2429–2445; c) G. Bottari, G. de La Torre, D. M. Guldi, T. Torres, *Chem. Rev.* **2010**, *110*, 6768–6816; d) C. Wang, H. Dong, W. Hu, Y. Liu, D. Zhu, *Chem. Rev.* **2011**, *111*, 2208–2267; e) M. R. Wasielewski, *Acc. Chem. Res.* **2009**, *42*, 1910–1921.
[3] a) F. Würthner, Z. Chen, F. J. M. Hoeben, P. Osswald, C. You, P. Jonkheijm, J. von Herrikhuyzen, A. P. H. J. Schenning, P. van der Schoot, E. W. Meijer, E. Beckers, S. Meskers, R. A. J. Janssen, *J. Am. Chem. Soc.* **2004**, *126*, 10611–10618; b) A. Kira, T. Umeyama, Y. Matano, K. Yoshida, S. Isoda, J. K. Park, D. Kim, H. Imahori, *J. Am. Chem. Soc.* **2009**, *131*, 3198–3200; c) F. G. Brunetti, C. Romero-Nieto, J. López-Andarias, C. Atienza, J. L. López, D. M. Guldi, N. Martín, *Angew. Chem. Int. Ed.* **2013**, *52*, 2180–2184; *Angew. Chem.* **2013**, *125*, 2236–2240.

[4] a) J. L. Delgado, P.-A. Bouit, S. Filippone, M. A. Herranz, N. Martín, *Chem. Commun.* **2010**, *46*, 4853 – 4865; b) D. M. Guldi, I. Zilbermann, G. Anderson, A. Li, D. Balbinot, N. Jux, M. Hatzimarinaki, A. Hirsch, M. Prato, *Chem. Commun.* **2004**, 726 – 727; c) O. Vostrowsky, A. Hirsch, *Chem. Rev.* **2006**, *106*, 5191 – 5207; d) T. Nagamachi, Y. Takeda, K. Nakayama, S. Minakata, *Chem. Eur. J.* **2012**, *18*, 12035 – 12045; e) M. Lenes, S. W. Shelton, A. B. Sieval, D. F. Kronholm, J. C. Hummelen, P. W. M. Blom, *Adv. Funct. Mater.* **2009**, *19*, 3002 – 3007; f) Y.-W. Wang, W. Zhang, X.-C. Ai, J.-P. Zhang, X.-F. Wang, J. Kido, *J. Phys. Chem. C* **2013**, *117*, 25898 – 25907; g) F. B. Kooistra, J. Knol, F. Kastenberg, L. M. Popescu, W. J. H. Verhees, J. M. Kroon, J. C. Hummelen, *Org. Lett.* **2007**, *9*, 551 – 554; h) S. S. Gayathri, M. Wielopolski, E. M. Pérez, G. Fernández, L. Sánchez, R. Viruela, E. Ortí, D. M. Guldi, N. Martín, *Angew. Chem. Int. Ed.* **2009**, *48*, 815 – 819; *Angew. Chem.* **2009**, *121*, 829 – 834; i) D. M. Guldi, B. M. Illescas, C. Atienza, M. Wielopolski, N. Martín, *Chem. Soc. Rev.* **2009**, *38*, 1587 – 1597; j) K. Yoosaf, J. Iehl, I. Nierengarten, M. Hmadeh, A.-M. Albrecht-Gary, J.-F. Nierengarten, N. Armaroli, *Chem. Eur. J.* **2014**, *20*, 223 – 231.

[5] M. Urbani, J. Iehl, I. Osinska, R. Louis, M. Holler, J.-F. Nierengarten, *Eur. J. Org. Chem.* **2009**, 3715 – 3725.

[6] Y. Zhang, Y. Matsuo, C.-Z. Li, H. Tanaka, E. Nakamura, *J. Am. Chem. Soc.* **2011**, *133*, 8086 – 8089.

[7] a) A. Varotto, N. D. Treat, J. Jo, C. G. Shuttle, N. A. Batara, F. G. Brunetti, J. H. Seo, M. L. Chabinyc, C. J. Hawker, A. J. Heeger, F. Wudl, *Angew. Chem. Int. Ed.* **2011**, *50*, 5166 – 5169; *Angew. Chem.* **2011**, *123*, 5272 – 5275; b) G.-W. Wang, Y.-M. Lu, Z.-X. Chen, *Org. Lett.* **2009**, *11*, 1507 – 1510.

[8] T. E. Kang, H.-H. Cho, C.-H. Cho, K.-H. Kim, H. Kang, M. Lee, S. Lee, B. S. Kim, C. Im, B. J. Kim, *ACS Appl. Mater. Interfaces* **2013**, *5*, 861 – 868.

[9] a) R. Fitzner, E. Reinold, A. Mishra, E. Mena-Osteritz, H. Ziehlke, C. Körner, K. Leo, M. Riede, M. Weil, O. Tsaryova, A. Weiß, C. Uhrich, M. Pfeiffer, P. Bäuerle, *Adv. Funct. Mater.* **2011**, *21*, 897 – 910; b) Y.-J. Cheng, S.-H. Yang, C.-S. Hsu, *Chem. Rev.* **2009**, *109*, 5868 – 5923; c) M. Turbiez, P. Frère, M. Allain, C. Videlot, J. Ackermann, J. Roncali, *Chem. Eur. J.* **2005**, *11*, 3742 – 3752; d) W. Li, H. E. Katz, A. J. Lovinger, J. G. Laquindanum, *Chem. Mater.* **1999**, *11*, 458 – 465; e) B. P. Karsten, L. Viani, J. Gierschner, J. Cornil, R. A. J. Janssen, *J. Phys. Chem. A* **2009**, *113*, 10343 – 10350; f) A. Mishra, C.-Q. Ma, P. Bäuerle, *Chem. Rev.* **2009**, *109*, 1141 – 1276; g) A. Mishra, P. Bäuerle, *Angew. Chem. Int. Ed.* **2012**, *51*, 2020 – 2067; *Angew. Chem.* **2012**, *124*, 2060 – 2109.

[10] a) N. Sakai, A. L. Sisson, T. Bürgi, S. Matile, *J. Am. Chem. Soc.* **2007**, *129*, 15758 – 15759; b) R. S. K. Kishore, O. Kel, N. Banerji, D. Emery, G. Bollot, J. Mareda, A. Gomez-Casado, P. Jonkheijm, J. Huskens, P. Maroni, M. Borkovec, E. Vauthey, N. Sakai, S. Matile, *J. Am. Chem. Soc.* **2009**, *131*, 11106 – 11116.

[11] N. Sakai, M. Lista, O. Kel, S. Sakurai, D. Emery, J. Mareda, E. Vauthey, S. Matile, *J. Am. Chem. Soc.* **2011**, *133*, 15224 – 15227.

[12] a) E.-K. Bang, G. Gasparini, G. Molinard, A. Roux, N. Sakai, S. Matile, *J. Am. Chem. Soc.* **2013**, *135*, 2088 – 2091; b) E.-K. Bang, M. Lista, G. Sforazzini, N. Sakai, S. Matile, *Chem. Sci.* **2012**, *3*, 1752 – 1763.

[13] a) M. Lista, J. Areephong, N. Sakai, S. Matile, *J. Am. Chem. Soc.* **2011**, *133*, 15228 – 15231; b) E. Orentas, M. Lista, N.-T. Lin, N. Sakai, S. Matile, *Nat. Chem.* **2012**, *4*, 746 – 750.

[14] N. Sakai, S. Matile, *J. Am. Chem. Soc.* **2011**, *133*, 18542 – 18545.

[15] A. Bolag, H. Hayashi, P. Charbonnaz, N. Sakai, S. Matile, *ChemistryOpen* **2013**, *2*, 55 – 57.

[16] J. Areephong, E. Orentas, N. Sakai, S. Matile, *Chem. Commun.* **2012**, *48*, 10618 – 10620.

[17] G. Sforazzini, E. Orentas, A. Bolag, N. Sakai, S. Matile, *J. Am. Chem. Soc.* **2013**, *135*, 12082 – 12090.

[18] See Supporting Information.

[19] M. Morisue, N. Haruta, D. Kalita, Y. Kobuke, *Chem. Eur. J.* **2006**, *12*, 8123 – 8135.

[20] J. Mišek, A. Vargas Jentzsch, S. Sakurai, D. Emery, J. Mareda, S. Matile, *Angew. Chem. Int. Ed.* **2010**, *49*, 7680 – 7683; *Angew. Chem.* **2010**, *122*, 7846 – 7849.

[21] Y. Yang, F. Arias, L. Echegoyen, L. P. F. Chibante, S. Flanagan, A. Robertson, L. J. Wilson, *J. Am. Chem. Soc.* **1995**, *117*, 7801 – 7804.

[22] A. Wilson, G. Gasparini, S. Matile, *Chem. Soc. Rev.* **2014**, *43*, 1948 – 1962.

